J. Fluid Mech. (2009), *vol.* 631, *pp.* 103–125.
doi:10.1017/S0022112009007204 Printed in the United Kingdom

Time-dependent water-wave scattering by arrays of cylinders and the approximation of near trapping

MICHAEL H. MEYLAN[1]† AND RODNEY EATOCK TAYLOR[2]

[1]Department of Mathematics, The University of Auckland, New Zealand

[2]Department of Engineering Science, Oxford University, UK

(Received 16 February 2008 and in revised form 19 February 2009)

We consider the solution in the time domain of water-wave scattering by arrays of bottom-mounted cylinders. It has already been shown that near trapping occurs for certain arrangements of cylinders and we are especially focused on this phenomenon. We begin with the well-known single-frequency solution to the problem of a group of cylinders, and the extension of this solution to complex frequencies. It has been shown that singularities (scattering frequencies or resonances) occur for certain values of the complex frequency and these singularities are associated with the near-trapped mode. We show that it is possible to approximate the solution near these singularities, and produce a modal shape which is associated with the near-trapped mode. We then consider the time-dependent problem, beginning with the well-known incident plane wave packet solution. We also show how the problem of an arbitrary initial displacement can be found using the single-frequency solutions. This latter result relies on a special inner product which gives a generalized eigenfunction expansion (because the operator has a continuous spectrum). We then consider the approximation of the time-dependent motion using special mode shapes associated with the scattering frequencies. This approximation relies on the scattering frequencies lying close to the real axis. We present numerical results which show that this approximation is accurate for sufficiently large time.

1. Introduction

This paper is concerned with the phenomenon of near-trapping of waves, in particular, the near-trapping phenomena which was discovered by Evans & Porter (1997) for the case of bottom-mounted cylinders. Near-trapped modes appear in the frequency domain solution as large spikes in the response, and it is in this context that they were considered by Evans & Porter. In the time domain the near-trapped mode appears as a slowly decaying mode which has a characteristic oscillation and fall time, and this was investigated by Eatock Taylor *et al.* (2006). The phenomenon of near trapping is associated with the phenomenon of trapped modes, although near trapping is not associated with any non-uniqueness in the frequency domain solution for real frequencies. Trapped modes in the context of an unbounded domain for water waves have received considerable attention since their discovery by McIver (1996), and they have been found for many situations (McIver & McIver 1997; McIver 2000;

† Email address for correspondence: meylan@math.auckland.ac.nz

McIver & McIver 2006). A trapped mode is associated with the existence of a real eigenvalue of the governing operator, whereas the near-trapped mode is associated with a singularity of the analytic extension of the governing operator close to the real axis. Unlike a trapped mode, a near-trapped mode can be excited by an incident wave.

A near-trapped mode is associated with a scattering frequency (also called a resonance) close to the real axis. A scattering frequency is a pole of the analytic continuation of the scattering operator (or the resolvent). This means that the pole occurs for non-physical frequencies for which the scattered solution grows towards infinity (away from the scattering body). In practice, the scattering frequencies can usually be calculated by considering the formula for real values of frequencies, but allowing the frequency to be complex and finding values for which the operator is not invertible. For the case of bottom-mounted cylinders that is exactly what was done by Evans & Porter (1997). Finding the scattering frequencies can be numerically challenging, and various methods to find them have been proposed (Meylan & Gross 2003). Scattering frequencies occur in many linear scattering processes, not just linear water waves. In the context of water waves, they have been investigated by Hazard & Lenoir (1993) and Hazard & Lenoir (2002) for the case of arbitrary two-dimensional bodies (although calculations were presented only for special cases), and by Meylan (2002) where the theory was connected with Lax–Phillips scattering and it was shown that the time-domain solution could be represented exactly as a sum over the scattering frequencies. This is only possible because for the problem considered, a floating elastic plate, the water depth was assumed shallow. Associated with the scattering frequencies is a mode shape, similar to an eigenfunction. The simple problem considered here, scattering by bottom-mounted cylinders, reduces to scattering by disks with Neumann boundary conditions for the two-dimensional Helmholtz equation. This avoids many of the difficulties associated with the analytic continuation, because there is only a single parameter, the wavenumber, which needs to be extended to complex values and the analytic continuation is therefore relatively simple.

The solution method in the time domain for arbitrary initial displacements (as opposed to a long-crested incident wave group) can be expanded in the frequency domain solutions using the *generalized eigenfunction* method. This method goes back to the work of Povzner (1953); Ikebe (1960); Wilcox (1975), and it has been used recently by Hazard & Lenoir (2002); Meylan (2002); Hazard & Loret (2007*a*); Hazard & Meylan (2007) for various water-wave problems. The generalized eigenfunction method works for certain types of operators which are self-adjoint, but which have a continuous spectrum. We therefore require a generalization of our notion of eigenfunction to functions which have infinite energy. The generalized eigenfunction expansion method is not an approximation and it provides an alternative to other time-domain methods, such as the memory-effect method and the time-dependent Green function method. The usual method to connect the scattering frequencies with the long-time behaviour is through the *singularity expansion method* (SEM), which is the method used by Hazard & Loret (2007*b*). In the SEM the solution is found using the Laplace transform, and the Bromwich contour integral is deformed (using the same analytic extension of the resolvent) to pass around the contribution from the scattering frequencies. We present here a new method in which the generalized eigenfunction expansion is connected to the expansion over the scattering frequencies. The time-domain solution using the scattering frequencies is an approximation which has a range of validity. For short times it is invalid because the solution is dominated by

short-lived effects. For medium times (computable times), if the scattering frequencies lie close to the real axis, the approximate solution will give good agreement with the full solution. In the long time, the response will be dominated by the very slowest decaying terms, which are described for a bobbing cylinder in Ursell (1964); Maskell & Ursell (1970). The importance of these very long-time terms remains an open question, and it is not considered in the present work.

The outline of the paper is as follows. In § 2 we introduce the governing equations for the array. In § 3 we discuss the eigenanalysis and give an approximate formula to predict the response shape at the near-trapped mode. Application of the approximation to the time-domain analysis of wave scattering by the array is discussed in § 4. This section contains a number of results which extend and explain what was found in Evans & Porter (1997). We give the well-known formulas for the case of an incident long-crested plane wave group, and we develop the formula for the case of an arbitrary forcing. The formula for the arbitrary case is derived using a generalized eigenfunction expansion. We then show that we can approximate the solution in the time domain by using the response shape (and complex response frequency) for large time. This gives a powerful predictive tool, as well as a clear explanation for the exponential rise and fall time which has been observed for these near-trapped modes. Section 5 is a brief summary of the paper.

2. Equations for N_c bottom-mounted cylinders

We consider the case of N_c bottom-mounted cylinders, of radius a_l, centred at (x_l, y_l) in water of constant finite depth H. The Cartesian coordinate system (x, y, z) has its origin on the mean free surface, with z pointing upwards. We define $\boldsymbol{x} = (x, y)$. The problem is linearized and the time-dependent equations are given by

$$\Delta \Psi (\boldsymbol{x}, z, t) = 0, \quad \boldsymbol{x} \in \Omega, \tag{2.1}$$

$$\partial_n \Psi = 0, \quad \boldsymbol{x} \in \partial\Omega, \tag{2.2}$$

$$\partial_n \Psi = 0, \quad z = -H, \tag{2.3}$$

where Ψ is the velocity potential, ∂_n is the normal derivative, Ω is the fluid domain and $\partial\Omega$ is the boundary of the fluid domain and the wetted cylinder walls. At the free surface $z = 0$ we have the kinematic condition

$$\partial_t \zeta = \partial_n \Psi, \quad z = 0, \tag{2.4}$$

where ζ is the surface displacement and t is time. The dynamic condition (the linearized Bernoulli equation) is

$$\partial_t \Psi = -\zeta, \quad z = 0. \tag{2.5}$$

Note that we have non-dimensionalized these equations with respect to a length scale L (which is arbitrary) and a time scale $\sqrt{L/g}$ so that gravity is unity.

2.1. *Frequency domain*

We can transform the equations in the time domain to the equations in the frequency domain by setting all time dependence to be $\mathrm{e}^{-\mathrm{i}\omega t}$ so that we can write

$$\Psi (\boldsymbol{x}, z, t) = \hat{\Psi} (\boldsymbol{x}, z, \omega)\, \mathrm{e}^{-\mathrm{i}\omega t} \quad \text{and} \quad \zeta (\boldsymbol{x}, t) = \hat{\zeta} (\boldsymbol{x}, \omega)\, \mathrm{e}^{-\mathrm{i}\omega t}. \tag{2.6}$$

This is equivalent to a Fourier transform in time of the equations.

Equations (2.1)–(2.5) become

$$\Delta\hat{\Psi}(\boldsymbol{x},z,\omega) = 0, \quad \boldsymbol{x} \in \Omega, \tag{2.7}$$

$$\partial_n\hat{\Psi} = 0, \quad \boldsymbol{x} \in \partial\Omega, \tag{2.8}$$

$$\partial_n\hat{\Psi} = 0, \quad z = -H, \tag{2.9}$$

$$-\mathrm{i}\omega\hat{\zeta} = \partial_n\hat{\Psi}, \quad z = 0, \tag{2.10}$$

and

$$\mathrm{i}\omega\hat{\Psi} = \hat{\zeta}, \quad z = 0. \tag{2.11}$$

Furthermore, because the cylinders extend to the seabed, the depth dependence can be removed by separation of variables and we can write the velocity potential as

$$\hat{\Psi}(\boldsymbol{x},z,\omega) = \phi(\boldsymbol{x},k)\,\psi(z), \tag{2.12}$$

where

$$\psi(z) = \frac{\cosh(k(z+H))}{\cosh kH}, \tag{2.13}$$

and k is the positive real solution of the dispersion equation

$$\omega^2 = k\tanh kH. \tag{2.14}$$

We also note that there are only propagating modes in this problem and the evanescent modes are zero. In what follows, both the variables k and ω will play an important role and we will need to use both. We assume that $k \geqslant 0$ and that $k(\omega) = k(-\omega)$. We also take $\omega(k)$ as the positive solution of (2.14).

We now consider the case when the system is excited by an incident wave. Usually, the incident wave is assumed to be a plane wave, but in what follows we will need to consider more general incident waves of the form $J_n(kr)\mathrm{e}^{\mathrm{i}n\theta}$. The equation for $\phi(\boldsymbol{x})$ is

$$\Delta\phi + k^2\phi = 0, \quad \boldsymbol{x} \in \bar{\Omega}, \tag{2.15}$$

$$\partial_n\phi = 0, \quad \boldsymbol{x} \in \partial\bar{\Omega}, \tag{2.16}$$

where $\bar{\Omega}$ is the free surface of the fluid domain and $\partial\bar{\Omega}$ is the boundary of the free surface and cylinders. We also require the Sommerfeld radiation boundary condition, which will be applied when we write down the expansion for the velocity potential.

The problem of calculating the wave diffraction by bottom-mounted cylinders permits a very efficient solution based on the Kagemoto & Yue (1986) interaction analysis. This theory is for arbitrary bodies, and the simplified equations for bottom mounted cylinders were given in Linton & Evans (1990). The theory is based on representing the incident and scattered wave around each body in the local eigenfunction expansion (in cylindrical coordinates), and mapping these from one body to another using Graf's addition theorem for Bessel functions (Abramowitz & Stegun 1970). As this theory is well-known, and has been used extensively, we will only summarize the equations.

We write the total potential as the sum of the incident potential and a scattered potential as

$$\phi(\boldsymbol{x},k) = \phi^{In}(\boldsymbol{x},k) + \phi^{s}(\boldsymbol{x},k). \tag{2.17}$$

The scattered potential $\phi^s(\boldsymbol{x}, k)$ we write as the sum of scattered waves centred at each of the N_c cylinders in the local coordinate system of each cylinder,

$$\phi^s(\boldsymbol{x}, k) = \sum_{j=1,}^{N_c} \sum_{m=-\infty}^{\infty} A_m^j H_m^{(1)}(kr_j) \mathrm{e}^{\mathrm{i}m\theta_j}, \tag{2.18}$$

where r_j and θ_j are the cylindrical coordinates of point $\boldsymbol{x}$ in the local coordinates of cylinder j, and $H_m^{(1)}(kr_j)$ is a Hankel function of the first kind (Abramowitz & Stegun 1970). We write the incident wave in the local coordinate system of cylinder l as

$$\phi^{In}(\boldsymbol{x}, k) = \sum_{m=-\infty}^{\infty} D_m^l J_m(kr_l) \mathrm{e}^{\mathrm{i}m\theta_l}, \tag{2.19}$$

and we will show how to determine D_m^l shortly. We now consider the lth cylinder and map all the scattered waves from the other cylinders using Graf's addition theorem to incident waves in the local coordinate system of cylinder l. This gives us

$$\phi(\boldsymbol{x}, k) = \sum_{m=-\infty}^{\infty} D_m^l J_m(kr_l) \mathrm{e}^{\mathrm{i}m\theta_l} + \sum_{m=-\infty}^{\infty} A_m^l H_m^{(1)}(kr_l) \mathrm{e}^{\mathrm{i}m\theta_l} \tag{2.20}$$

$$+ \sum_{m=-\infty}^{\infty} \left(\sum_{j=1, j\neq l}^{N_c} \sum_{\nu=-\infty}^{\infty} A_m^j H_{\nu-m}^{(1)}(kR_{jl}) \mathrm{e}^{\mathrm{i}(\nu-m)\varphi_{jl}} \right) J_m(kr_l) \mathrm{e}^{\mathrm{i}m\theta_l}, \tag{2.21}$$

where (R_{jl}, φ_{jl}) are the polar coordinates of the mean centre position of cylinder l in the local coordinates of cylinder j. The boundary condition $\partial_n \phi = 0$ at the boundary of cylinder l (where $r_l = a_l$) gives us

$$\sum_{m=-\infty}^{\infty} D_m^l J_m'(ka_l) \mathrm{e}^{\mathrm{i}m\theta_l} + \sum_{m=-\infty}^{\infty} A_m^l H_m^{(1)\prime}(ka_l) \mathrm{e}^{\mathrm{i}m\theta_l} \tag{2.22}$$

$$+ \sum_{m=-\infty}^{\infty} \left(\sum_{j=1, j\neq l}^{N_c} \sum_{\nu=-\infty}^{\infty} A_m^j H_{\nu-m}^{(1)}(kR_{jl}) \mathrm{e}^{\mathrm{i}(\nu-m)\varphi_{jl}} \right) J_m'(ka_l) \mathrm{e}^{\mathrm{i}m\theta_l} = 0. \tag{2.23}$$

Since this holds for each angle we obtain

$$D_m^l J_m'(ka_l) + A_m^l H_m^{(1)\prime}(ka_l) + \left(\sum_{j=1, j\neq l}^{N_c} \sum_{\nu=-\infty}^{\infty} A_m^j H_{\nu-m}^{(1)}(kR_{jl}) \mathrm{e}^{\mathrm{i}(\nu-m)\varphi_{jl}} \right) J_m'(ka_l) = 0, \tag{2.24}$$

which simplifies to

$$\frac{J_m'(ka_l)}{H_m^{(1)\prime}(ka_l)} \left[\sum_{j=1, j\neq l}^{N_c} \sum_{\tau=-\infty}^{\infty} A_\tau^j H_{\tau-\nu}^{(1)}(kR_{jl}) \mathrm{e}^{\mathrm{i}(\tau-m)\varphi_{jl}} \right] + A_m^l = -\frac{J_m'(ka_l)}{H_m^{(1)\prime}(ka_l)} D_m^l. \tag{2.25}$$

For the case of a plane incident wave

$$\phi^{In} = \mathrm{e}^{\mathrm{i}k(x\cos\chi + y\sin\chi)}, \tag{2.26}$$

where χ is the incident wave angle,

$$D_\nu^l = \mathrm{e}^{\mathrm{i}k(x_l\cos\chi + y_l\sin\chi)} \mathrm{e}^{\mathrm{i}\nu(\pi/2-\chi)}. \tag{2.27}$$

For the case of a cylindrical incident wave

$$\phi^{In} = J_n(kr) \mathrm{e}^{\mathrm{i}n\theta}, \tag{2.28}$$

we calculate D_m^l from Graf's addition theorem (Yilmaz & Incecik 1998)

$$J_n(kr)\mathrm{e}^{\mathrm{i}n\theta} = \sum_{\nu=-\infty}^{\infty} J_\nu(kr_l)J_{\nu-n}(kR_l)\mathrm{e}^{\mathrm{i}(\nu-n)(\pi-\vartheta_l)}\mathrm{e}^{\mathrm{i}\nu\theta_l}, \tag{2.29}$$

where (R_l, ϑ_l) is the coordinates of the centre of lth cylinder in radial coordinates centred at the origin. Therefore,

$$D_\nu^l = \sum_{\nu=-\infty}^{\infty} J_{\nu-n}(kR_l)\mathrm{e}^{\mathrm{i}(\nu-n)(\pi-\vartheta_l)}. \tag{2.30}$$

3. Scattering frequencies

We begin with the truncated version of (2.25), and develop our theory from this approximation. An equivalent theory could be developed using the full equations and the truncation could be introduced later when a numerical approximation was required. The truncated version of (2.25), approximated by a finite number of modes, is

$$\frac{J_m'(ka_l)}{H_m^{(1)\prime}(ka_l)}\left[\sum_{j=1,j\neq l}^{N_c}\sum_{\tau=-M}^{M} A_\tau^j H_{\tau-\nu}^{(1)}(kR_{jl})\mathrm{e}^{\mathrm{i}(\tau-m)\varphi_{jl}}\right] + A_m^l = -\frac{J_m'(ka_l)}{H_m^{(1)\prime}(ka_l)}D_m^l, \quad 1 \leqslant l \leqslant N_c. \tag{3.1}$$

This can be written as a matrix equation for the unknown vector $\boldsymbol{a}$ of coefficients A_ν^l as

$$\boldsymbol{M}(k)\boldsymbol{a} + \boldsymbol{a} = \boldsymbol{f}(k), \tag{3.2}$$

where $\boldsymbol{M}$ is the matrix which follows from the left-hand side of (2.25) and $\boldsymbol{f}$ is the vector which follows from the right-hand side. Equation (3.2) is the equation to calculate the scattering numerically for real frequencies. The solution to the truncated scattering problem is given by

$$\boldsymbol{a} = (\boldsymbol{I} + \boldsymbol{M}(k))^{-1}\boldsymbol{f}(k), \tag{3.3}$$

where $\boldsymbol{I}$ is the identity matrix.

We now consider (2.25) for complex k. We find that the matrix $\boldsymbol{I} + \boldsymbol{M}(k)$ has a zero eigenvalue for a set of discrete points $k = k_p$ in the lower half of the complex plane (which is equivalent to the matrix $\boldsymbol{M}(k_p)$ having an eigenvalue of -1). From equation (3.3) for $k = k_p$, $\boldsymbol{a}$ will be singular, i.e. the system will have infinite response. The values k_p are called scattering frequencies. $(\boldsymbol{I} + \boldsymbol{M}(k))^{-1}$ is the resolvent and the scattering frequencies are the singularities of the analytic continuation of the resolvent. There is no requirement for the analytic continuation of the matrix $\boldsymbol{M}(k)$ to be meromorphic, i.e. we may have arbitrary branch cuts, accumulation points of zeros, etc. Even in very well-behaved situations (such as Meylan 2002) there was an infinite number of zeros. Determining the properties of the analytic continuation in the general case remains challenging. It is possible to represent the solution in the time domain as a sum over the scattering frequencies plus other contributions, and this method is known as the SEM. We also note that, due to causality, the scattering frequencies only occur in the lower half-plane. This is because we have used $\mathrm{e}^{-\mathrm{i}\omega t}$ time dependence (with positive ω). For certain very special situations in the general wave scattering problem, a real value of the scattering frequency k_p can occur which corresponds to a trapped mode. For the case of scattering by a finite array of cylinders in an unbounded domain

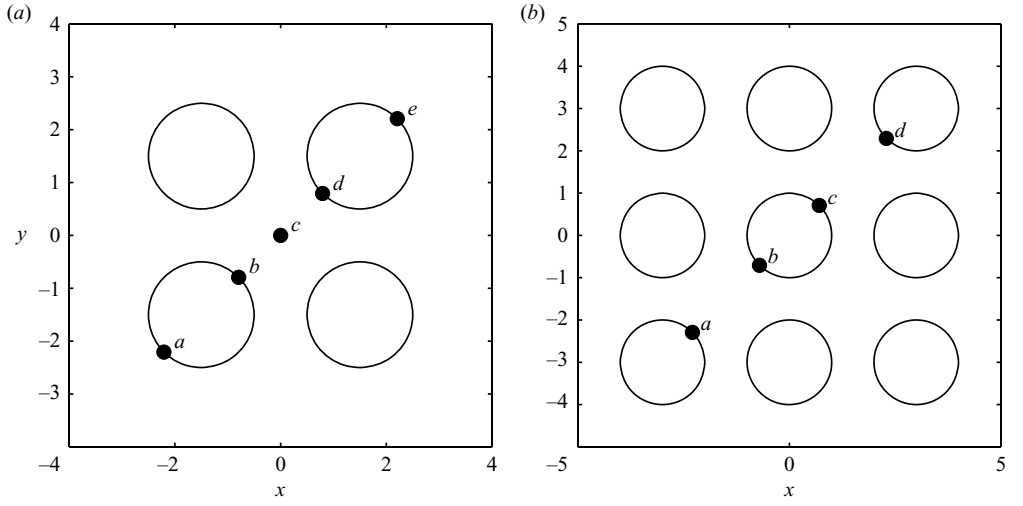

FIGURE 1. The two arrangements of cylinders and the points at which we will calculate the displacement.

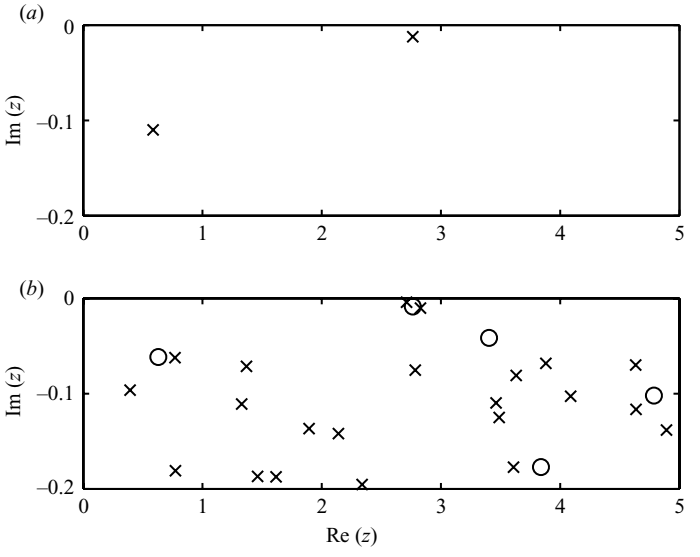

FIGURE 2. The location of the scattering frequencies in the region of the complex plane given by $\{z \in \mathbb{C},\ -0.2 < \mathrm{Im}(z) < 0,\ 0 < \mathrm{Re}(z) < 5\}$: (*a*) is for four and (*b*) is for nine cylinders. The single roots are marked with a $\times$ and the double roots with an $\circ$.

trapped modes have never been found. However, there are situations of near trapping where a scattering frequency occurs close to the real axis, as was shown by Evans & Porter (1997). In that work, the near trapping occurred especially for symmetric arrangements of identical cylinders.

3.1. *Results for the scattering frequencies*

For our numerical calculations we consider two arrangements of cylinders, a grid of four cylinders and a grid of nine cylinders. The cylinders have radius 1 and the centres of the cylinders are spaced 3 apart. These are shown in figure 1. Figure 2 shows the

location of the scattering frequencies in the subset of the complex plane given by $\{z \in \mathbb{C},\ -0.2 < \mathrm{Im}(z) < 0,\ 0 < \mathrm{Re}(z) < 5\}$ for the two arrangements. There is one scattering frequency close to the real axis for the four cylinders at $2.7641–0.0122i$ and there are three scattering frequencies close to the real axis for nine cylinders at $2.7114–0.0041i$ (single root), $2.8284–0.0102i$ (single root) and $2.7635–0.0086i$ (double root). Note that the real parts of these values are all very similar.

3.2. *Calculation of the residues*

Suppose we have a scattering frequency at a complex wavenumber k_p. The scattering frequency k_p is associated with an eigenvector $\boldsymbol{u}_{k_p}$ with the property that

$$(\boldsymbol{I} + \boldsymbol{M}(k_p))\boldsymbol{u}_{k_p} = 0. \tag{3.4}$$

Near a simple pole we can write the inverse of $\boldsymbol{I} + \boldsymbol{M}(k)$ as

$$(\boldsymbol{I} + \boldsymbol{M}(k))^{-1} \approx \frac{\mathbf{A}(k_p)}{k - k_p}, \tag{3.5}$$

where $\mathbf{A}(k_p)$ is the residue which is connected with a projection onto the eigenspace associated with $\boldsymbol{u}_{k_p}$. The expression for $\mathbf{A}(k)$ follows from Hazard & Loret (2007*b*, Theorem 3.5, p. 934) using a result due to Steinberg (1968), when the eigenspace has dimension one. The case of a double root will be presented separately for reasons of clarity. In practice, the double roots situation is important because in problems with symmetry (which we consider here) double roots do occur. Near the simple root k_p it can be shown that

$$(\boldsymbol{I} + \boldsymbol{M}(k))^{-1} \approx \frac{\boldsymbol{u}_{k_p}\boldsymbol{u}^*_{k^*_p}}{\boldsymbol{u}^*_{k^*_p}\boldsymbol{M}^{(1)}\boldsymbol{u}_{k_p}(k - k_p)}, \tag{3.6}$$

where $\boldsymbol{u}^*_{k^*_p}$, written as a row vector, is the eigenvector of the adjoint of $\boldsymbol{M}$ with eigenvalue -1 (which occurs at k^*_p). The action of the right-hand side is to multiple a column vector by the row vector $\boldsymbol{u}^*_{k^*_p}$ to produce a scaler and then to multiple this by the column vector $\boldsymbol{u}_{k_p}$ normalized by the denominator (which is also a scalar). $\boldsymbol{M}^{(1)}$ is the derivative of $\boldsymbol{M}$ at k_p given by

$$\boldsymbol{M}^{(1)} = \frac{\mathrm{d}}{\mathrm{d}k}\,\boldsymbol{M}(k)|_{k=k_p}\,. \tag{3.7}$$

Therefore,

$$\mathbf{A}(k_p) = \frac{\boldsymbol{u}_{k_p}\boldsymbol{u}^*_{k^*_p}}{\boldsymbol{u}^*_{k^*_p}\boldsymbol{M}^{(1)}\boldsymbol{u}_{k_p}}. \tag{3.8}$$

3.2.1. *Double root formula*

In the case of double roots we assume that there are two linearly independent eigenvectors associated with k_p. The case where there is only a single eigenvector would definitely be exceptional, and we have not encountered this situation in any numerical results. Such a situation would also imply more complicated time-dependent behaviour, which may make the case physically impossible.

We let $\boldsymbol{u}_{k_p}$ and $\boldsymbol{v}_{k_p}$ be two linearly independent eigenvectors and we choose the two eigenfunctions of the adjoint $\boldsymbol{u}^*_{k^*_p}$ and $\boldsymbol{v}^*_{k^*_p}$ with the properties that $\boldsymbol{u}_{k_p}\boldsymbol{v}^*_{k^*_p} = \boldsymbol{v}_{k_p}\boldsymbol{u}^*_{k^*_p} = 0$. In general, we have to be careful about choosing $\boldsymbol{u}_{k_p}$ and $\boldsymbol{v}_{k_p}$, but in the examples considered here where the double root arises from the body symmetry, any linear

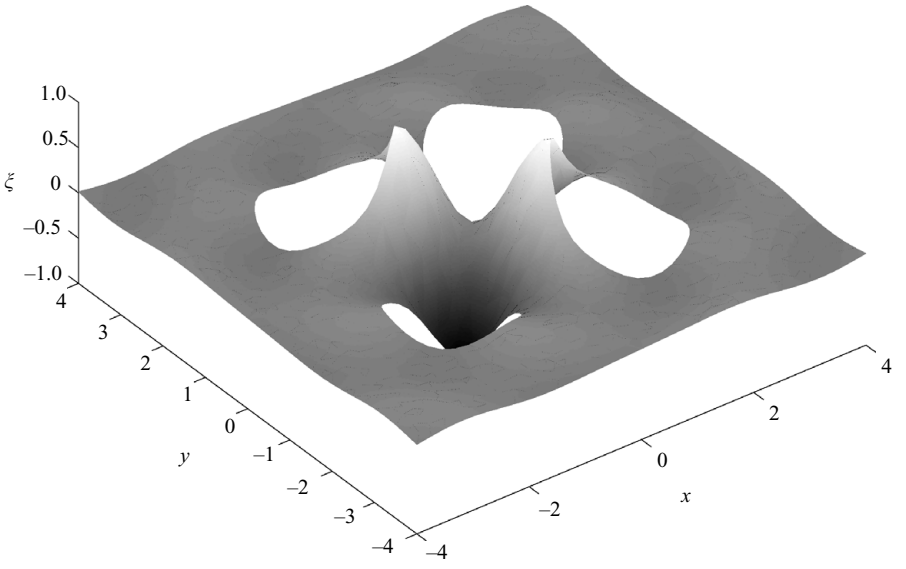

FIGURE 3. The near-trapped mode for four cylinders associated with the scattering frequency at 2.7641–0.0122i.

independent vectors are fine. Then

$$\mathbf{A}(k_p) = \frac{\boldsymbol{u}_{k_p}\boldsymbol{u}^*_{k^*_p}}{\boldsymbol{u}^*_{k^*_p}\boldsymbol{M}^{(1)}\boldsymbol{u}_{k_p}} + \frac{\boldsymbol{v}_{k_p}\boldsymbol{v}^*_{k^*_p}}{\boldsymbol{v}^*_{k^*_p}\boldsymbol{M}^{(1)}\boldsymbol{v}_{k_p}}. \tag{3.9}$$

Triple or higher roots can obviously be treated in a similar fashion.

3.3. *Approximation of the frequency-domain solution.*

Near the scattering frequency we can approximate the scattered wave ϕ^s given by (3.3), using the approximation derived in (3.8) or (3.9) (although we will not consider this latter case explicitly). Thus near the point k_p the approximation is

$$\boldsymbol{a}(k) \approx \frac{\boldsymbol{u}^*_{k^*_p}\boldsymbol{f}(k_p)}{\boldsymbol{u}^*_{k^*_p}\boldsymbol{M}^{(1)}\boldsymbol{u}_{k_p}(k-k_p)}\boldsymbol{u}_{k_p}. \tag{3.10}$$

We observe that we can extend $\boldsymbol{f}$ to complex values from the definition given in the right-hand side of (3.1).

3.4. *Results for the approximation in the frequency domain*

We can find the mode shape associated with each of the scattering frequencies from

$$U_{k_p}(\boldsymbol{x}) = \sum_{j=1}^{N_c}\sum_{m=-N}^{N} u^j_m H^{(1)}_m(k_p r_j)\mathrm{e}^{\mathrm{i}m\theta_j}, \tag{3.11}$$

where k_p is the scattering frequency and u^j_m are the values corresponding to the eigenvector $\boldsymbol{u}_{k_p}$. Note that we are using the notation $\boldsymbol{u}$ for the vector of coefficients and U for the corresponding function. The mode shapes are not the eigenfunctions of any operator, and they grow as r tends to infinity (because k_p is in the lower complex half-plane).

Figures 3 and 4 show the surface displacement associated with the eigenvector $\boldsymbol{u}_{k_p}$. We plot $\mathrm{Re}\{U_{k_p}\}$ and in movies 1–5 we show the surface displacement for a

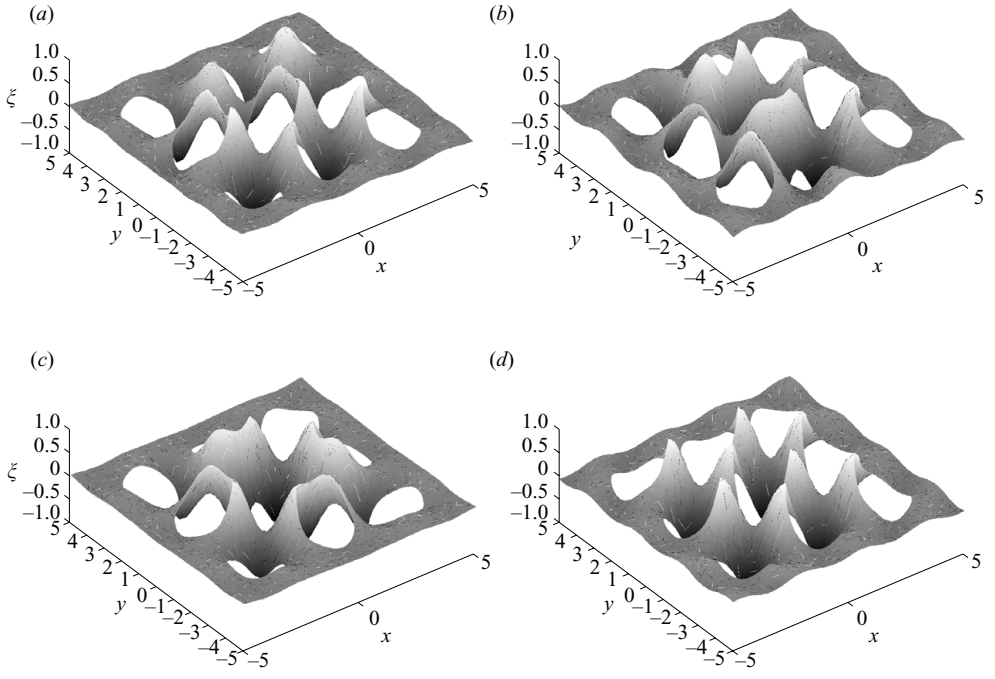

FIGURE 4. The near-trapped mode for nine cylinders associated with the scattering frequency at 2.7114–0.0041i (a), 2.7635–0.0086i (b) and (c), and 2.8284–0.0102i (d).

complete period, $\mathrm{Re}\{U_{k_p} \mathrm{e}^{-\mathrm{i}\omega_p t}\}$. These are the near-trapped modes. Their growth towards infinity is quite slow for scattering frequencies close to the real axis, which is why the growth is not apparent in the figures. We can see that the modal shape for nine cylinders is approximately composed of various combinations of the modal shapes for four cylinders, either in phase or out of phase with each other.

4. Time-domain calculations

The solution in the frequency domain can be used to construct the solution in the time domain. This was shown by Eatock Taylor *et al.* (2006) and discussed further by Eatock Taylor & Meylan (2007) for the case of a plane incident wave which is initially far from the body. However, when we consider an initial displacement which is non-zero around the cylinders, the problem is of much greater complexity. The solution then requires a generalized eigenfunction expansion and a special inner product.

4.1. *Calculation in the time domain for a plane incident wave*

Consider the case when the cylinders are excited by a long-crested incident wave travelling in the χ direction with arbitrary initial profile $f(x\cos\chi + y\sin\chi)$ when the wave is far from the body for large negative time. If we denote

$$\hat{f}(k) = \int_{-\infty}^{\infty} f(s)\,\mathrm{e}^{\mathrm{i}ks}\,\mathrm{d}s, \tag{4.1}$$

then we can express the time-dependent motion by

$$\Phi(\boldsymbol{x},t)=\frac{1}{2\pi}\int_0^\infty \hat{f}(k)\left(\mathrm{e}^{\mathrm{i}k(x\cos\chi+y\sin\chi)}+\phi^s(\boldsymbol{x},k)\right)\mathrm{e}^{-\mathrm{i}\omega t}\,\mathrm{d}k + \frac{1}{2\pi}\int_0^\infty \hat{f}(-k)\left(\mathrm{e}^{-\mathrm{i}k(x\cos\chi+y\sin\chi)}+(\phi^s(\boldsymbol{x},k))^*\right)\mathrm{e}^{\mathrm{i}\omega t}\,\mathrm{d}k, \quad (4.2)$$

where $\Phi(\boldsymbol{x},t)$ is the surface potential (we could find the full potential Ψ by including the ψ term in the integral) and ω is related to k through the dispersion equation (2.14). This formula is derived from the principle of superposition of the solutions for each frequency. We find $\phi^s(\boldsymbol{x},k)$, by solving (2.25) for the incident potential given by $\mathrm{e}^{\mathrm{i}k(x\cos\chi+y\sin\chi)}$ (i.e. using (2.27)). Provided that $f(t)$ is real (so that $\hat{f}(-k)=\hat{f}(k)^*$),we can write

$$\Phi(\boldsymbol{x},t)=\mathrm{Re}\left[\frac{1}{\pi}\int_0^\infty \hat{f}(k)\left(\mathrm{e}^{\mathrm{i}k(x\cos\chi+y\sin\chi)}+\phi^s(\boldsymbol{x},k)\right)\mathrm{e}^{-\mathrm{i}\omega t}\,\mathrm{d}k\right]. \quad (4.3)$$

4.2. *Calculation in the time domain for arbitrary initial conditions*

Calculation of the displacement for arbitrary initial conditions is a more challenging problem, and seems not to have been undertaken hitherto. Unlike the case of a plane incident wave we need to begin with the equations in the time domain (2.4)–(2.5). We introduce the operator $\mathbf{G}$ which maps the free surface potential Φ to the potential Ξ throughout the fluid domain. We define $\mathbf{G}\Phi=\Xi$, and obtain Ξ by solving

$$\Delta\Xi(\boldsymbol{x},z)=0 \quad \boldsymbol{x}\in\Omega, \quad (4.4)$$

$$\partial_n\Xi=0, \quad \boldsymbol{x}\in\partial\Omega, \quad (4.5)$$

$$\partial_n\Xi=0, \quad z=-H, \quad (4.6)$$

$$\Xi=\Phi, \quad z=0. \quad (4.7)$$

We introduce the operator $\partial_n\mathbf{G}$ which maps the free surface potential to the normal derivative of potential at the surface (the Dirichlet-to-Neumann map) which is given by

$$\partial_n\mathbf{G}\Phi=\partial_n\Xi|_{z=0}. \quad (4.8)$$

We can therefore write (2.1)–(2.5) as the following:

$$\mathrm{i}\partial_t\begin{pmatrix}\Phi\\-\mathrm{i}\zeta\end{pmatrix}=\begin{pmatrix}0&1\\\partial_n\mathbf{G}&0\end{pmatrix}\begin{pmatrix}\Phi\\-\mathrm{i}\zeta\end{pmatrix}. \quad (4.9)$$

The evolution operator

$$\mathscr{A}=\begin{pmatrix}0&1\\\partial_n\mathbf{G}&0\end{pmatrix} \quad (4.10)$$

is symmetric in an inner product space equipped with the following inner product

$$\left\langle\begin{pmatrix}\Phi\\-\mathrm{i}\zeta\end{pmatrix},\begin{pmatrix}\Upsilon\\-\mathrm{i}\eta\end{pmatrix}\right\rangle_{\mathscr{H}}=\int_\Omega(\nabla\mathbf{G}\Phi)(\nabla\mathbf{G}\Upsilon)^*\,\mathrm{d}\Omega+\int_{\bar{\Omega}}(-\mathrm{i}\zeta)(-\mathrm{i}\eta)^*\,\mathrm{d}\bar{\Omega}. \quad (4.11)$$

Note that this inner product is an expression for the energy and it follows that, since the equations of motion preserve energy, our operator $\mathscr{A}$ which gives the evolution of energy must be symmetric. We can prove this mathematically by using Green's

second identity:

$$\int_\Omega (\nabla \mathbf{G}\Phi)(\nabla \mathbf{G}\Upsilon)\,\mathrm{d}\Omega = \int_{\bar{\Omega}} (\partial_n \mathbf{G}\Phi)\,\Upsilon\,\mathrm{d}\bar{\Omega} - \int_\Omega (\Delta \mathbf{G}\Phi)(\mathbf{G}\Upsilon)\,\mathrm{d}\Omega$$
$$= \int_{\bar{\Omega}} (\partial_n \mathbf{G}\Phi)\,\Upsilon\ \mathrm{d}\bar{\Omega}, \tag{4.12}$$

(the last line following since $\Delta \mathbf{G}\Phi = 0$). Therefore,

$$\left\langle \mathscr{A}\begin{pmatrix}\Phi\\ -\mathrm{i}\zeta\end{pmatrix}, \begin{pmatrix}\Upsilon\\ -\mathrm{i}\eta\end{pmatrix}\right\rangle_{\mathscr{H}} = \int_\Omega (-\mathrm{i}\nabla \mathbf{G}\zeta)(\nabla \mathbf{G}\Upsilon)^*\,\mathrm{d}\Omega + \int_{\bar{\Omega}} (\partial_n \mathbf{G}\Phi)(-\mathrm{i}\eta)^*\,\mathrm{d}\bar{\Omega}$$
$$= \int_{\bar{\Omega}} (-\mathrm{i}\zeta)(\partial_n \mathbf{G}\Upsilon)^*\,\mathrm{d}\bar{\Omega} + \int_\Omega (\nabla \mathbf{G}\Phi)(-\mathrm{i}\nabla \mathbf{G}\eta)^*\,\mathrm{d}\Omega$$
$$= \left\langle \begin{pmatrix}\Phi\\ -\mathrm{i}\zeta\end{pmatrix}, \mathscr{A}\begin{pmatrix}\Upsilon\\ -\mathrm{i}\eta\end{pmatrix}\right\rangle_{\mathscr{H}}. \tag{4.13}$$

We now make the non-trivial assumption that the inner product space is a Hilbert space and the operator is self-adjoint. The proof of this is technical, and requires very precise definitions of which functions are in the Hilbert space. It is the property of self-adjointness which we need for our generalized eigenfunction expansion.

4.2.1. *Generalized eigenfunctions of* $\mathscr{A}$

The generalized eigenfunctions of $\mathscr{A}$ satisfy

$$\mathscr{A}\begin{pmatrix}\Phi\\ -\mathrm{i}\zeta\end{pmatrix} = \omega\begin{pmatrix}\Phi\\ -\mathrm{i}\zeta\end{pmatrix}. \tag{4.14}$$

Equation (4.14) is nothing more than (2.7)–(2.11). This means that to solve for the generalized eigenfunctions of $\mathscr{A}$ we need to solve the frequency domain equations, and the frequency ω is exactly the eigenvalue.

We write the eigenfunctions of $\mathscr{A}$ (with eigenvalue ω) in the vector form

$$\vec{\phi}_n(\boldsymbol{x},\omega) = \begin{cases} \begin{pmatrix}\phi_n(\boldsymbol{x}, k(\omega))\\ \omega\phi_n(\boldsymbol{x}, k(\omega))\end{pmatrix}, & \omega > 0,\\ \begin{pmatrix}(\phi_n(\boldsymbol{x}, k(\omega)))^*\\ \omega(\phi_n(\boldsymbol{x}, k(\omega)))^*\end{pmatrix}, & \omega < 0,\end{cases} \tag{4.15}$$

where the subscript n represents counting over an index (and not the normal derivative). $\phi_n(\boldsymbol{x}, k)$ is the solution for an incident wave of the form $J_n(kr)\,\mathrm{e}^{\mathrm{i}n\theta}$. That is

$$\phi_n(\boldsymbol{x}, k) = J_n(kr)\,\mathrm{e}^{\mathrm{i}n\theta} + \sum_{j=1}^{N_c}\sum_{m=-\infty}^{\infty} A_m^j H_m^{(1)}(kr_j)\mathrm{e}^{\mathrm{i}m\theta_j}, \tag{4.16}$$

where A_m^j are found by solving (2.25) with D_m^l given by (2.30). We know that the generalized eigenfunctions are orthogonal so that

$$\langle \vec{\phi}_n^+(\boldsymbol{x},\omega_1), \vec{\phi}_m^+(\boldsymbol{x},\omega_2)\rangle_{\mathscr{H}} = \Lambda_n(\omega_1)\,\delta(\omega_1-\omega_2)\,\delta_{mn}, \tag{4.17}$$

but we need to determine the normalizing function $\Lambda_n(\omega_1)$. This is achieved by using the result that the generalized eigenfunctions satisfy the same normalizing condition with and without the scattering terms. This result, the proof of which is quite technical, is well known and has been shown for many different situations. The original proof

was for Schrödinger's equation and was due to Povzner (1953); Ikebe (1960). A proof for the case of Helmholtz equation (our problem if the depth is shallow) was given by Wilcox (1975). Recently, the proof was given for water waves by Hazard & Lenoir (2002); Hazard & Loret (2007*a*). In none of these papers were any calculations made. Furthermore, they avoided using delta functions so that no expression equivalent to (4.17) appears.

We now assume that the generalized eigenfunctions satisfy the same normalizing condition with and without the scattering terms and also that we can remove the scattering cylinders when calculating the normalizing condition. This gives us the following (assuming that $\omega_1 \geqslant 0$ and $\omega_2 \geqslant 0$)

$$\begin{aligned}
\langle \vec{\phi}_n^+(\boldsymbol{x}, k(\omega_1)), \vec{\phi}_m^+(\boldsymbol{x}, k(\omega_2))\rangle_{\mathscr{H}} &= \left\langle \begin{pmatrix} J_n(k_1 r)\,\mathrm{e}^{\mathrm{i}n\theta} \\ \omega_1 J_n(k_1 r)\mathrm{e}^{\mathrm{i}n\theta} \end{pmatrix}, \begin{pmatrix} J_m(k_2 r)\mathrm{e}^{\mathrm{i}m\theta} \\ \omega_2 J_m(k_2 r)\mathrm{e}^{\mathrm{i}m\theta} \end{pmatrix} \right\rangle_{\mathscr{H}} \\
&= \int_{\Omega'} (\nabla \mathbf{G} J_n(k_1 r)\mathrm{e}^{\mathrm{i}n\theta})(\nabla \mathbf{G} J_m(k_2 r)\mathrm{e}^{\mathrm{i}m\theta})^* \,\mathrm{d}\Omega' \\
&\quad + \int_{\bar{\Omega}'} (\omega_1 J_n(k_1 r)\mathrm{e}^{\mathrm{i}m\theta})(\omega_2 J_m(k_2 r)\mathrm{e}^{\mathrm{i}m\theta})^* \,\mathrm{d}\bar{\Omega}' \\
&= \int_{\bar{\Omega}'} (J_n(k_1 r)\mathrm{e}^{\mathrm{i}n\theta})(\partial_n \mathbf{G} J_m(k_2 r)\mathrm{e}^{\mathrm{i}m\theta})^* \,\mathrm{d}\bar{\Omega}' \\
&\quad + \omega_1\omega_2 \int_{\bar{\Omega}'} (J_n(k_1 r)\mathrm{e}^{\mathrm{i}n\theta})(J_n(k_2 r)\mathrm{e}^{\mathrm{i}m\theta})^* \,\mathrm{d}\bar{\Omega}' \\
&= \int_{\bar{\Omega}'} (J_n(k_1 r)\mathrm{e}^{\mathrm{i}n\theta})(\omega_m^2 J_m(k_2 r)\mathrm{e}^{\mathrm{i}m\theta})^* \,\mathrm{d}\bar{\Omega}' \\
&\quad + \omega_1\omega_2 \int_{\bar{\Omega}'} (J_n(k_1 r)\mathrm{e}^{\mathrm{i}n\theta})(J_n(k_2 r)\mathrm{e}^{\mathrm{i}m\theta})^* \,\mathrm{d}\bar{\Omega}' \\
&= 4\pi \frac{\omega_2^2}{k_1} \delta_{nm} \delta(k_1 - k_2) \\
&= 4\pi \frac{\omega_2^2}{k_1} \delta_{nm} \delta(\omega_1 - \omega_2) \left.\frac{\mathrm{d}\omega}{\mathrm{d}k}\right|_{\omega=\omega_1},
\end{aligned} \tag{4.18}$$

where Ω' is the entire domain with the cylinders removed and $\bar{\Omega}'$ is the free surface of this domain. The last steps follow from the Bessel transform and from the change of coordinates expression for delta functions. This result allows us to calculate the expansion of the potential in generalized eigenfunctions. The negative ω case is almost identical, except we need to evaluate the derivative at $\omega = -\omega_1$ since we have defined k to be positive.

4.2.2. *Expansion in generalized eigenfunctions*

The solution on the free surface can be expanded as

$$\begin{pmatrix} \Phi(\boldsymbol{x}, t) \\ -\mathrm{i}\zeta(\boldsymbol{x}, t) \end{pmatrix} = \int_{-\infty}^{\infty} k \left\{ \sum_{n=-\infty}^{\infty} f_n(\omega)\, \vec{\phi}_n(\boldsymbol{x}, \omega) \right\} \mathrm{e}^{-\mathrm{i}\omega t} \mathrm{d}\omega. \tag{4.19}$$

We include the weighting term k (which is always positive) because it is required for the orthogonality relation for Bessel functions, and including it here makes subsequent formulas simpler. The time-domain solution throughout the fluid can be calculated in a straightforward way, by including the depth-dependence term ψ.

If we take the inner product (assuming $\omega \geqslant 0$) we obtain

$$\left\langle \begin{pmatrix} \Phi(\boldsymbol{x},0) \\ -\mathrm{i}\zeta(\boldsymbol{x},0) \end{pmatrix}, \vec{\phi}_n(\boldsymbol{x},k) \right\rangle_{\mathscr{H}} = 4\pi f_n(\omega)\,\omega^2 \frac{\mathrm{d}\omega}{\mathrm{d}k}. \tag{4.20}$$

This gives the following expression for $f_n(\omega)$ for $\omega \geqslant 0$,

$$\begin{aligned} f_n(\omega) &= \frac{1}{4\pi\omega^2}\frac{\mathrm{d}k}{\mathrm{d}\omega}\int_{\Omega} \nabla\mathbf{G}\Phi(\boldsymbol{x},0)\,(\nabla\mathbf{G}\phi_n(\boldsymbol{x},k))^*\,\mathrm{d}\Omega + \frac{1}{4\pi\omega^2}\frac{\mathrm{d}k}{\mathrm{d}\omega}\int_{\bar{\Omega}} -\mathrm{i}\zeta(\boldsymbol{x},0)(\omega\phi_n(\boldsymbol{x},k))^*\mathrm{d}\bar{\Omega} \\ &= \frac{1}{4\pi\omega^2}\frac{\mathrm{d}k}{\mathrm{d}\omega}\int_{\bar{\Omega}} \Phi(\boldsymbol{x},0)\,(\partial_n\mathbf{G}\phi_n(\boldsymbol{x},k))^*\,\mathrm{d}\bar{\Omega} - \frac{i}{4\pi\omega^2}\frac{\mathrm{d}k}{\mathrm{d}\omega}\int_{\bar{\Omega}} \omega\zeta(\boldsymbol{x},0)\,(\phi_n(\boldsymbol{x},k))^*\,\mathrm{d}\bar{\Omega} \\ &= \frac{1}{4\pi\omega^2}\frac{\mathrm{d}k}{\mathrm{d}\omega}\int_{\bar{\Omega}} \Phi(\boldsymbol{x},0)(\omega^2\phi_n(\boldsymbol{x},k))^*\mathrm{d}\bar{\Omega} - \frac{i}{4\pi\omega^2}\frac{\mathrm{d}k}{\mathrm{d}\omega}\int_{\bar{\Omega}} \omega\zeta(\boldsymbol{x},0)\,(\phi_n(\boldsymbol{x},k))^*\,\mathrm{d}\bar{\Omega} \\ &= \frac{1}{4\pi\omega}\frac{\mathrm{d}k}{\mathrm{d}\omega}\int_{\bar{\Omega}} [\omega\Phi(\boldsymbol{x},0) - \mathrm{i}\zeta(\boldsymbol{x},0)]\,(\phi_n(\boldsymbol{x},k))^*\,\mathrm{d}\bar{\Omega}. \end{aligned} \tag{4.21}$$

We can derive a similar formula for $\omega < 0$ and we obtain the result that $f_n(\omega) = (f_n(-\omega))^*$ for $\omega < 0$. This allow us to write the expansion (4.19) as

$$\begin{pmatrix} \Phi(\boldsymbol{x},t) \\ -\mathrm{i}\zeta(\boldsymbol{x},t) \end{pmatrix} = \mathrm{Re}\left\{ \int_0^{\infty} 2k \left\{ \sum_{n=-\infty}^{\infty} f_n(\omega)\,\vec{\phi}_n(\boldsymbol{x}, k(\omega)) \right\} \mathrm{e}^{-\mathrm{i}\omega t}\,\mathrm{d}\omega \right\}. \tag{4.22}$$

If we take the case when $\zeta(\boldsymbol{x},0) = 0$ and change variables so the integration is over k the formula simplifies and we obtain

$$\Phi(\boldsymbol{x},t) = \mathrm{Re}\left\{ \int_0^{\infty} k \left\{ \sum_{n=-\infty}^{\infty} \left(\frac{1}{2\pi}\int_{\bar{\Omega}} \Phi(\boldsymbol{x},0)\,(\phi_n(\boldsymbol{x},k))^*\,\mathrm{d}\bar{\Omega} \right) \phi_n(\boldsymbol{x},k) \right\} \mathrm{e}^{-\mathrm{i}\omega t}\,\mathrm{d}k \right\}. \tag{4.23}$$

If $\Phi(\boldsymbol{x},0) = 0$, we have

$$\zeta(\boldsymbol{x},t) = \mathrm{Re}\left\{ \int_0^{\infty} k \left\{ \sum_{n=-\infty}^{\infty} \left(\frac{1}{2\pi}\int_{\bar{\Omega}} \zeta(\boldsymbol{x},0)\,(\phi_n(\boldsymbol{x},k))^*\,\mathrm{d}\bar{\Omega} \right) \phi_n(\boldsymbol{x},k) \right\} \mathrm{e}^{-\mathrm{i}\omega t}\,\mathrm{d}k \right\}. \tag{4.24}$$

It is clear from (4.23) and (4.24) that the evolution of an initial potential without any displacement is equivalent to the evolution of the same initial displacement without any initial potential.

The theory above can be simplified by making the assumption that the water depth is shallow. With the non-dimensionalization we have adopted this means that $\omega = \sqrt{H}k$. The equations in this case are given in the Appendix.

4.3. *Approximation of the time-domain solution.*

4.3.1. *Plane incident wave*

We consider now only the part of (4.2) which comes from the scattered wave, and we ignore the plane wave (which is unaffected by the cylinders), and we assume that there are P poles close to the real axis at k_p, $p = 1, \ldots, P$. Then we have

$$\begin{aligned} \Phi(\boldsymbol{x},t) &= \mathrm{Re}\left[\frac{1}{\pi}\int_0^{\infty} \hat{f}(k)\left(\mathrm{e}^{\mathrm{i}k(x\cos\chi + y\sin\chi)} + \phi^s(\boldsymbol{x},k) \right) \mathrm{e}^{-\mathrm{i}\omega t}\,\mathrm{d}k \right] \\ &\approx \mathrm{Re}\left[\frac{1}{\pi}\int_0^{\infty} \hat{f}(k) \sum_{p=1}^{P} \left(\frac{\boldsymbol{u}_{k_p}^* \boldsymbol{f}(k_p)}{\boldsymbol{u}_{k_p}^* \boldsymbol{M}^{(1)} \boldsymbol{u}_{k_p}(k - k_p)} \right) U_{k_p}(\boldsymbol{x}) \mathrm{e}^{-\mathrm{i}\omega t}\,\mathrm{d}k \right], \end{aligned} \tag{4.25}$$

where $U_{k_p}(\boldsymbol{x})$ is given by (3.11) and we are also assuming that $\boldsymbol{u}^*_{k^*_p}$ have been chosen correctly according to (3.9) in the case when there is a repeated root. It is clear from the fact that we have ignored the incident wave solution that we are already considering only large t. We now assume that t is sufficiently large that we can further approximate this integral by closing the contour in the lower half-plane. There is then a contribution from the integral down the negative imaginary axis. We are neglecting the contributions from all other terms in ϕ^s and we also neglect the contribution from this integral as well. There is no obvious reason why the contribution from this integral needs to be small, nor that the contributions from the other poles can be ignored, except that for the case we consider here the scattering frequencies we do consider are very close to the real axis. Furthermore, the numerical results show that the contribution from the neglected term, for the examples considered here, is small. This leads to

$$\Phi(\boldsymbol{x}, t) \approx \mathrm{Re}\left[\sum_{p=1}^{P} -2\mathrm{i}\hat{f}(k_p)\left(\frac{\boldsymbol{u}^*_{k^*_p}\boldsymbol{f}(k_p)}{\boldsymbol{u}^*_{k^*_p}\boldsymbol{M}^{(1)}\boldsymbol{u}_{k_p}}\right) U_{k_p}(\boldsymbol{x})\mathrm{e}^{-\mathrm{i}\omega_p t}\right]. \tag{4.26}$$

Note that we can extend the definition of $\hat{f}$ to complex values using (4.1).

4.3.2. *Results for a plane incident wave group*

For our time-dependent results we will always assume the water is shallow, using the expressions given in the Appendix. This allows some simplifications in the computations, but it is done primarily to facilitate interpretation of the presented results, since there is no dispersion of the wave groups investigated. We also assume, following the Appendix, that $H = 1$. Figures 6 and 7 (and movies 6 and 7) show the free surface vertical displacement at the points shown in figure 1 for an incident plane wave group specified by

$$\hat{f}(k) = 2\sqrt{\pi}\mathrm{e}^{-4(k-k_0)^2}, \quad k \geqslant 0, \quad \text{and} \quad \hat{f}(k) = \hat{f}(-k)^*, \quad k < 0, \tag{4.27}$$

for $k_0 = 2.7635$. This value of k_0 for the four cylinder case corresponds to the real part of the scattering frequency which is very close to the real axis (see Figure 2*a*). As seen in figure 2(*b*), there are three scattering frequencies for nine cylinders whose real parts are close to the value $k_0 = 2.7635$, so we use this value in our investigations of both four cylinders and nine cylinders. A plot of this incident wave group is shown in figure 5(*a*). The group is compact and has a maximum value of unity. We consider the wave to be incident in the $\chi = \pi/4$ direction and we consider the free surface elevation at the points shown in figure 1. Figures 6 and 7 show results for four cylinders and nine cylinders, respectively, obtained from the generalized eigenfunction expansion and from the approximation by (4.26). In the case of four cylinders, one pole is included in the approximation; for the nine cylinders, the four poles close to $k_0 = 2.7635$ are used. We also show these solutions in movies 6 and 7. It is clear that once the wave group has passed, there is good agreement between the approximate theory and the true solution. There is a slow decay of the near-trapped mode, which is not apparent on these short time scales. For the nine cylinder case there is a beating of the response due to the existence of four modes of nearly the same frequency (see figure 7*b* for example). We will investigate this beating further when we consider the time-dependent solution for arbitrary initial conditions.

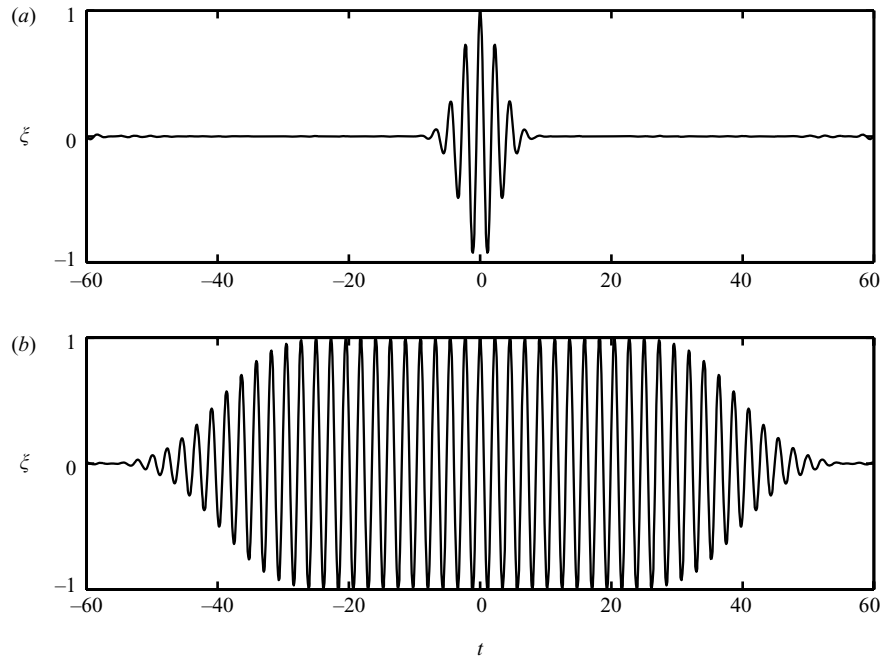

FIGURE 5. The incident undisturbed plane wave function given by (4.27) (*a*) and (4.28) (*b*).

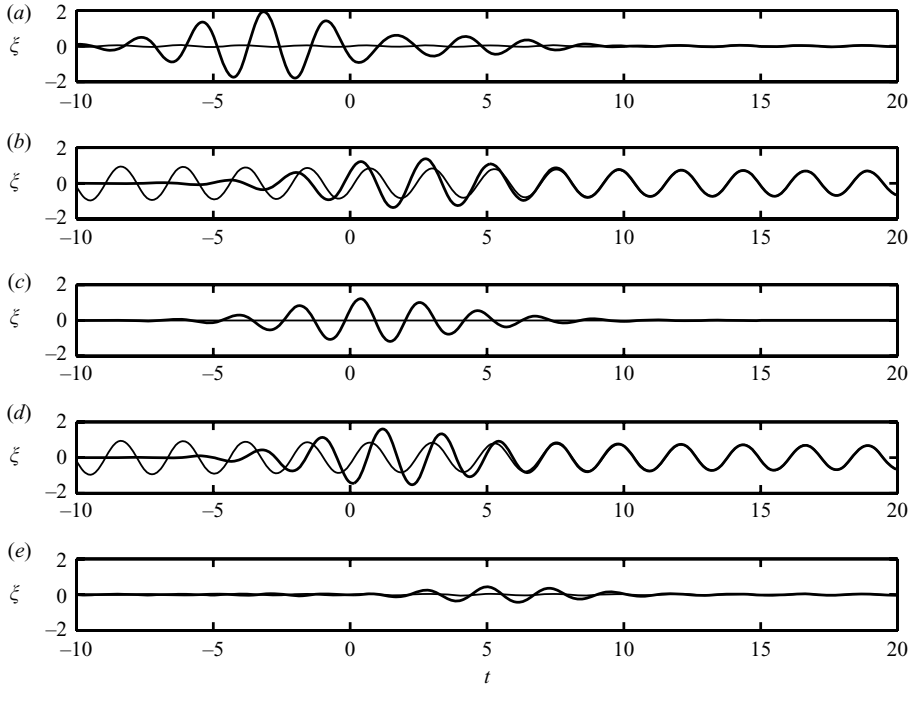

FIGURE 6. The true (thicker line) and approximate (thinner line) solution at points *a*–*e* near the four cylinders in figure 1, for a plane incident wave given by (4.27).

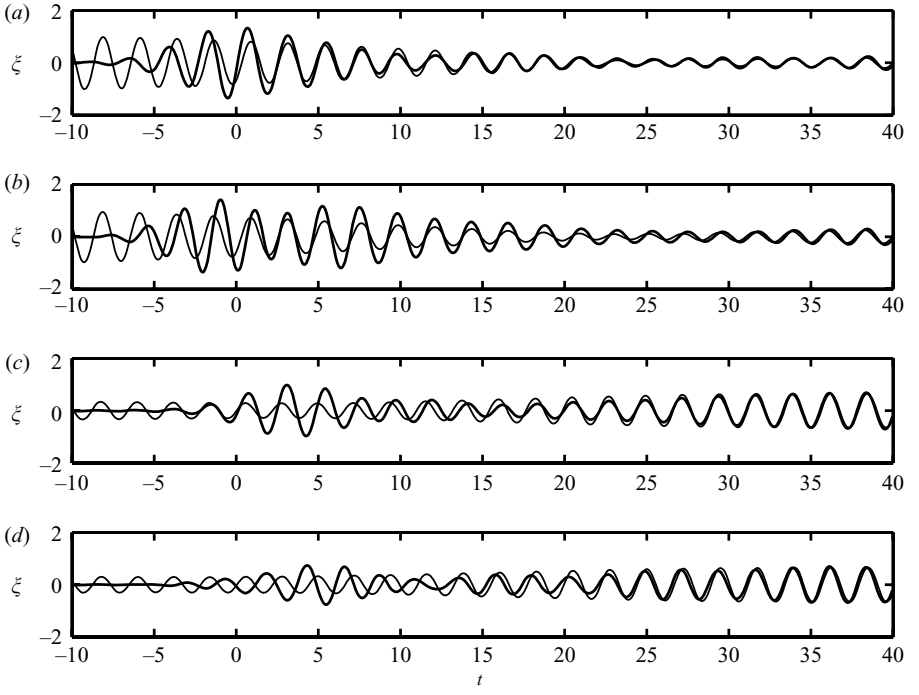

FIGURE 7. The true (thicker line) and approximate (thinner line) solution at points a–d near the nine cylinders in figure 1, for a plane incident wave given by (4.27).

We also consider a group given by

$$\hat{f}(k) = \frac{\sin(40(k-k_0))}{k-k_0} \mathrm{e}^{-20(k-k_0)^2}, \quad k \geqslant 0, \quad \text{and} \quad \hat{f}(k) = \hat{f}(-k)^*, \quad k < 0, \quad (4.28)$$

which corresponds to a much longer wave packet which is concentrated at the frequency k_0. The incident wave group is shown in figure 5(b), and the resulting free surface elevation at the points near the four cylinders in figure 8 (note the different ordinates in the subplots of elevation) and movie 8. This shows the buildup of energy as well as the subsequent decay. We have only plotted the approximate solution for $t > 0$. The difference between the displacement during the rise time and the saturation displacement follows an exponential decay. This pattern in the rise could be explained using a similar argument to the one developed here.

4.3.3. *Solution for arbitrary initial conditions*

We now consider the case when the initial conditions are arbitrary. To keep the presentation simple, we set the initial potential to zero so that displacement is given by (4.24). In the plane wave case there was only a single-incident wave direction so that we did not have to consider a sum over n. However, in all other regards the approximation proceeds exactly as before. We take

$$\phi_n(\boldsymbol{x}, k) = \sum_{p=1}^{P} \left(\frac{\boldsymbol{u}_{k_p}^* \boldsymbol{f}_n(k)}{\boldsymbol{u}_{k_p}^* \boldsymbol{M}^{(1)} \boldsymbol{u}_{k_p}(k-k_p)} \right) U_{k_p}(\boldsymbol{x}), \quad (4.29)$$

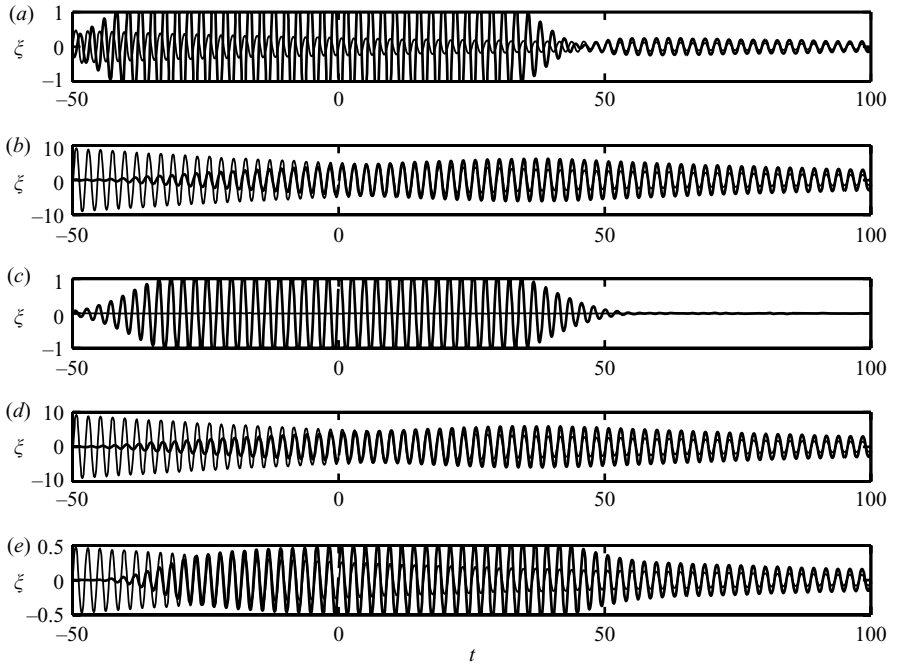

FIGURE 8. The true (thicker line) and approximate (thinner line) solution at points *a–e* near the four cylinders in figure 1, for a plane incident wave given by (4.28).

which leads to

$$\zeta(\boldsymbol{x},t) \approx \mathrm{Re}\left[\int_0^\infty k\left\{\sum_{n=-N}^{N}\left(\frac{1}{2\pi}\int_{\bar{\Omega}}\zeta(\boldsymbol{x},0)\left(\sum_{p=1}^{P}\left(\frac{\boldsymbol{u}_{k_p^*}^* \boldsymbol{f}_n(k)}{\boldsymbol{u}_{k_p^*}^* \boldsymbol{M}^{(1)} \boldsymbol{u}_{k_p}(k-k_p)}\right) U_{k_p}(\boldsymbol{x})\right)^* \mathrm{d}\bar{\Omega}\right)\right.\right.$$
$$\left.\left.\times\left(\sum_{q=1}^{P}\left(\frac{\boldsymbol{u}_{k_q^*}^* \boldsymbol{f}_n(k)}{\boldsymbol{u}_{k_q^*}^* \boldsymbol{M}^{(1)} \boldsymbol{u}_{k_q}(k-k_q)}\right) U_{k_q}(\boldsymbol{x})\right)\right\} \mathrm{e}^{-\mathrm{i}\omega t}\mathrm{d}k\right]$$
$$\approx \mathrm{Re}\left[\sum_{p=1}^{P}\frac{-\mathrm{i}k_p}{(k_p-k_p^*)}\sum_{n=-N}^{N}\left|\frac{\boldsymbol{u}_{k_p^*}^* \boldsymbol{f}_n(k_p)}{\boldsymbol{u}_{k_p^*}^* \boldsymbol{M}^{(1)} \boldsymbol{u}_{k_p}}\right|^2\left(\int_{\bar{\Omega}}\zeta(\boldsymbol{x},0)\left(U_{k_p}(\boldsymbol{x})\right)^* \mathrm{d}\bar{\Omega}\right) U_{k_p}(\boldsymbol{x})\mathrm{e}^{-\mathrm{i}\omega_p t}\right]. \tag{4.30}$$

Note that we can calculate $\boldsymbol{f}_n$ for complex values as we did for $\boldsymbol{f}$. Here we have derived the last expression by closing the contour in the lower half-plane and again ignoring the contribution from the imaginary axis. We have also assumed that the poles are sufficiently far apart that we can treat them separately, or that when poles are close together, they have come from the splitting of orthogonal poles and that they have retained this orthogonality enough to be approximated as orthogonal.

4.3.4. *Results for an arbitrary initial condition*

We present results for an initial distribution of the form

$$\xi = \mathrm{e}^{-2((x-0.5)^2+(y-0.5)^2)} + \mathrm{e}^{-2((x+0.5)^2+(y+0.5)^2)}. \tag{4.31}$$

This initial condition is shown in figure 9. The elevation at points near the cylinders is shown in figures 10–11 and we also show the solution in movies 9 and 10. The

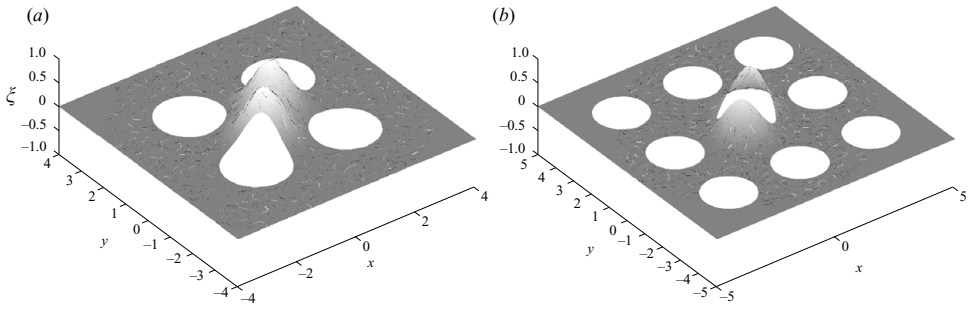

FIGURE 9. The initial condition given by (4.31) for four (*a*) and nine (*b*) cylinders.

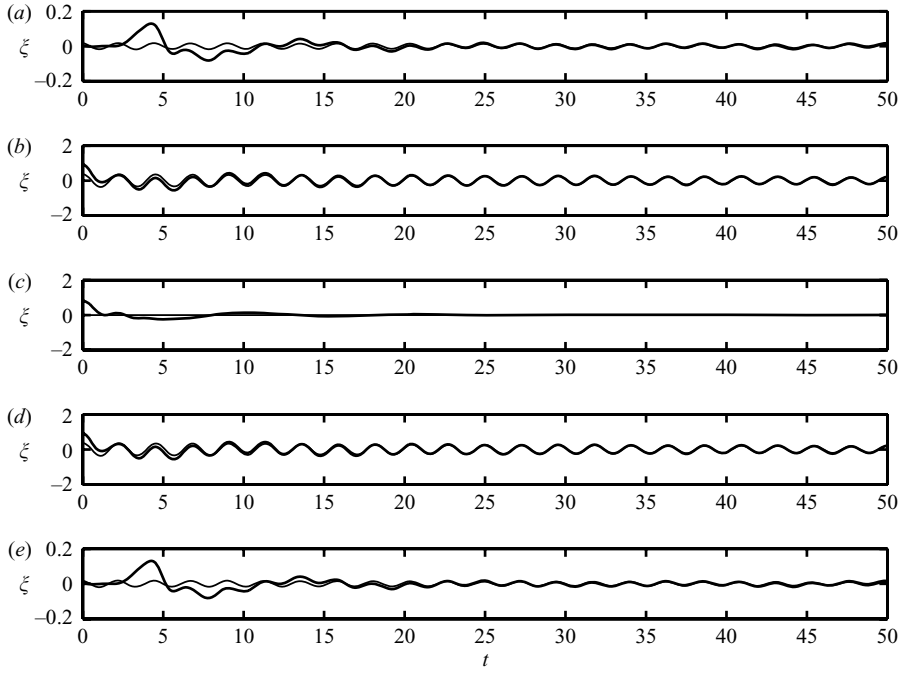

FIGURE 10. The true (thicker line) and approximate (thinner line) solution for the points *a*–*e* as shown in figure 1 for an incident displacement given by (4.31) for four cylinders.

true solution tends to the approximate solution after an initial period of time. The long-time solution shown for nine cylinders, plotted in figure 12, shows the beating effect of the four near-trapped modes (shown in figure 4) having close frequencies as shown in figure 2(*b*).

5. Summary

We have considered the problem of near trapping by arrays of vertical bottom-mounted cylinders. This problem has been well studied and it is relatively simple to determine the single-frequency solutions. We have shown that the solution in the time domain can be calculated from the single-frequency solutions. For the case of a plane incident wave from infinity this is straightforward, but for the case of an arbitrary

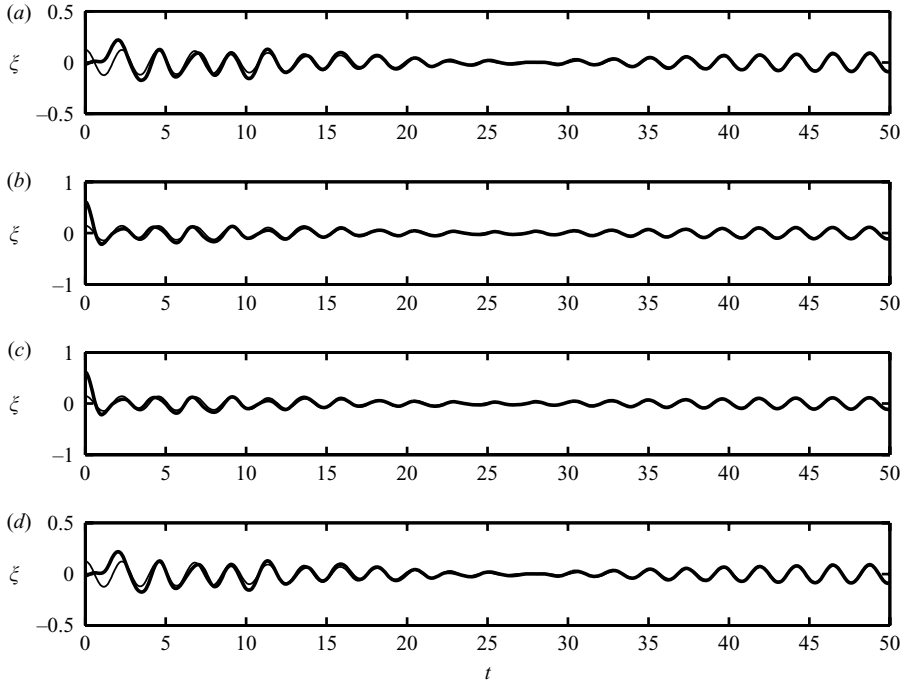

FIGURE 11. The true (thicker line) and approximate (thinner line) solution for the points *a–d* as shown in figure 1 for an incident displacement given by (4.31) for nine cylinders.

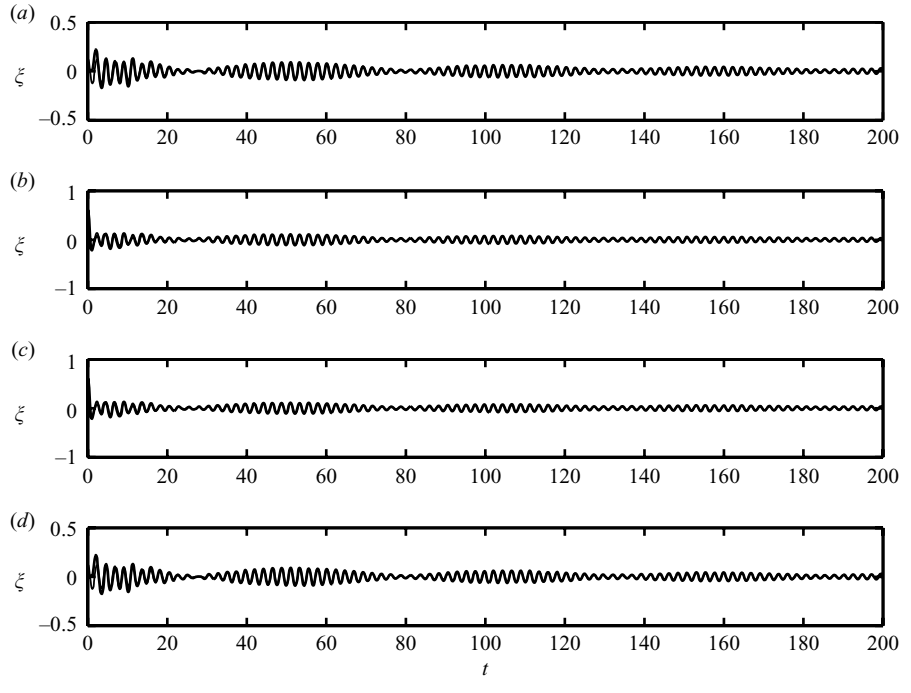

FIGURE 12. As in figure 11 except the time is from 0 to 200.

initial condition we require the use of a generalized eigenfunction expansion. It has previously been established that the near trapping is associated with a singularity in the analytic extension of the solution to the lower complex plane. We have shown here that there is also a mode associated with the singularity which is similar to an eigenfunction. We have shown that, by deforming the contour of integration given the generalized eigenfunction expansion, we can determine an approximate solution in terms of the near-trapped modes. We have given some numerical examples for arrangements of four and nine cylinders which show the validity of our approach.

The method outlined here could be extended to other situations. For example, the theoretical basis for the extension of the generalized eigenfunction expansion to floating bodies can be found in Hazard & Lenoir (2002). If a particular geometry has near-trapped modes, the method outlined to find the approximation should work exactly as described here.

This research was supported by Marsden grant UOO308 from the New Zealand government. We would also like to thank Dr Garry Tee for his editorial assistance.

Appendix. Shallow water

We present here the equations when the water depth is shallow. Because we have removed the depth dependence in the finite depth equations, the finite depth and shallow depth equations are almost identical. The only difference between (4.23) and (4.24) and the equations we will derive here is that for shallow water the dispersion equation (2.14) is $k = |\omega|/\sqrt{H}$ (i.e. there is no dispersion in shallow water). We further assume that $H = 1$ to simplify the equations we will derive. The equations satisfied by $\Phi(\boldsymbol{x}, t)$ for shallow water are the following:

$$\Delta\Phi = \partial_t \zeta, \quad \boldsymbol{x} \in \bar{\Omega}, \tag{A 1}$$

$$\partial_t \Phi = -\zeta, \quad \boldsymbol{x} \in \partial\bar{\Omega}. \tag{A 2}$$

We write the equations in the time domain as

$$\mathrm{i}\partial_t \begin{pmatrix} \Phi \\ -\mathrm{i}\zeta \end{pmatrix} = \begin{pmatrix} 0 & 1 \\ \Delta & 0 \end{pmatrix} \begin{pmatrix} \Phi \\ -\mathrm{i}\zeta \end{pmatrix}. \tag{A 3}$$

The evolution operator

$$\mathscr{A} = \begin{pmatrix} 0 & 1 \\ \Delta & 0 \end{pmatrix} \tag{A 4}$$

is symmetric in the inner product space with inner product given by

$$\left\langle \begin{pmatrix} \Phi \\ -\mathrm{i}\zeta \end{pmatrix}, \begin{pmatrix} \Upsilon \\ -\mathrm{i}\eta \end{pmatrix} \right\rangle_{\mathscr{H}} = \int_{\bar{\Omega}} \nabla\Phi \, (\nabla\Upsilon)^* \, \mathrm{d}\bar{\Omega} + \int_{\bar{\Omega}} -\mathrm{i}\zeta \, (-\mathrm{i}\eta)^* \, \mathrm{d}\bar{\Omega}. \tag{A 5}$$

As before we assume that the inner product space is a Hilbert space and the operator is self-adjoint. The generalized eigenfunctions of the operator are given by

$$\vec{\phi}_n(\boldsymbol{x}, \omega) = \begin{cases} \begin{pmatrix} \phi_n(\boldsymbol{x}, k(\omega)) \\ \omega\phi_n(\boldsymbol{x}, k(\omega)) \end{pmatrix}, & \omega > 0 \\ \begin{pmatrix} (\phi_n(\boldsymbol{x}, k(\omega)))^* \\ \omega\,(\phi_n(\boldsymbol{x}, k(\omega)))^* \end{pmatrix}, & \omega < 0 \end{cases}, \tag{A 6}$$

where $\phi_n(\boldsymbol{x}, k)$ are exactly as found previously. These satisfy the following orthogonality relations, assuming $\omega_1 \geqslant 0$ and $\omega_2 \geqslant 0$

$$\begin{aligned}\langle \vec{\phi}_n(\boldsymbol{x}, \omega_1), \vec{\phi}_m(\boldsymbol{x}, \omega_2) \rangle_{\mathscr{H}} &= \int_{\bar{\Omega}} \nabla\phi_n(\boldsymbol{x}, k_1)(\nabla\phi_m(\boldsymbol{x}, k_2))^* \, \mathrm{d}\bar{\Omega} + \int_{\bar{\Omega}} k_1\phi_n(\boldsymbol{x}, k_1)(k_2\phi_m(\boldsymbol{x}, k_2))^* \mathrm{d}\bar{\Omega} \\ &= \int_0^{2\pi} \int_0^{\infty} k_1 k_2 r J_n(k_1 r) \, \mathrm{e}^{\mathrm{i}n\theta} J_n(k_2 r) \, \mathrm{e}^{-\mathrm{i}m\theta} \, \mathrm{d}r \, \mathrm{d}\theta \\ &\quad + \int_0^{2\pi} \int_0^{\infty} k_1 k_2 r J_n(k_1 r) \, \mathrm{e}^{\mathrm{i}n\theta} J_n(k_2 r) \, \mathrm{e}^{-\mathrm{i}m\theta} \, \mathrm{d}r \mathrm{d}\theta \\ &= 4\pi\delta_{mn} k_1 \delta(k_1 - k_2) \\ &= 4\pi\delta_{mn}\omega_1 \delta(\omega_1 - \omega_2). \end{aligned} \tag{A 7}$$

The normalizing condition for negative ω is the same. The solution in the time domain is expanded in the waves $\vec{\phi}_n(\boldsymbol{x}, \omega)$:

$$\begin{pmatrix} \Phi(\boldsymbol{x}, t) \\ -\mathrm{i}\zeta(\boldsymbol{x}, t) \end{pmatrix} = \int_{\infty}^{\infty} k \left\{ \sum_{n=-\infty}^{\infty} f_n(k) \, \vec{\phi}_n(\boldsymbol{x}, \omega) \right\} \mathrm{e}^{-\mathrm{i}\omega t} \, \mathrm{d}\omega. \tag{A 8}$$

If we take the inner product we obtain

$$\left\langle \begin{pmatrix} \Phi(\boldsymbol{x}, 0) \\ -\mathrm{i}\zeta(\boldsymbol{x}, 0) \end{pmatrix}, \vec{\phi}(\boldsymbol{x}, \omega) \right\rangle_{\mathscr{H}} = 4\pi\omega^2 f_n(\omega). \tag{A 9}$$

This gives us the following expression for $f_n(\omega)$ for $\omega \geqslant 0$,

$$\begin{aligned} f_n(\omega) &= \frac{1}{4\pi k^2} \int_{\bar{\Omega}} \nabla\Phi(\boldsymbol{x}, 0)(\nabla\phi_n(\boldsymbol{x}, k))^* \, \mathrm{d}\bar{\Omega} + \frac{1}{4\pi k^2} \int_{\bar{\Omega}} -\mathrm{i}\zeta(\boldsymbol{x}, 0)(k\phi_n(\boldsymbol{x}, k))^* \, \mathrm{d}\bar{\Omega} \\ &= \frac{1}{4\pi k^2} \int_{\bar{\Omega}} \Phi(\boldsymbol{x}, 0)(-\Delta\phi_n(\boldsymbol{x}, k))^* \, \mathrm{d}\bar{\Omega} + \frac{1}{4\pi k} \int_{\bar{\Omega}} -\mathrm{i}\zeta(\boldsymbol{x}, 0)(\phi_n(\boldsymbol{x}, k))^* \, \mathrm{d}\bar{\Omega} \\ &= \frac{1}{4\pi} \int_{\bar{\Omega}} \Phi(\boldsymbol{x}, 0)(\phi_n(\boldsymbol{x}, k))^* \, \mathrm{d}\bar{\Omega} + \frac{1}{4\pi k} \int_{\bar{\Omega}} -\mathrm{i}\zeta(\boldsymbol{x}, 0)(\phi_n(\boldsymbol{x}, k))^* \, \mathrm{d}\bar{\Omega}. \end{aligned} \tag{A 10}$$

It can easily be shown that $f_n(\omega) = (f_n(-\omega))^*$ for $\omega < 0$. If we take the case when $\Phi(\boldsymbol{x}, 0) = 0$, then the formula simplifies and we obtain

$$\zeta(\boldsymbol{x}, t) = \mathrm{Re}\left\{ \int_0^{\infty} k \left\{ \sum_{n=-\infty}^{\infty} \left(\frac{1}{2\pi} \int_{\bar{\Omega}} -\mathrm{i}\zeta(\boldsymbol{x}, 0)(\phi_n(\boldsymbol{x}, k))^* \, \mathrm{d}\bar{\Omega} \right) \phi_n(\boldsymbol{x}, k) \right\} \mathrm{e}^{-\mathrm{i}kt} \mathrm{d}k \right\}, \tag{A 11}$$

where we have replaced ω by k. This is identical to (4.24) except there is no dispersion in this equation.

REFERENCES

Abramowitz, M. & Stegun, I. A. 1970 *Handbook of Mathematical Functions*. Dover.

Eatock Taylor, R. & Meylan, M. H. 2007 Theory of scattering frequencies applied to near-trapping by cylinders. In *22nd International Workshop on Water Waves and Floating Bodies,* pp. 73–76, Plitvice, Croatia.

Eatock Taylor, R., Zang, J., Bai, W. & Walker, D. A. G. 2006 Transients in wave diffraction by cylinders and cylinder arrays. *21st International Workshop on Water Waves and Floating Bodies,* pp. 37–40, Loughborough, UK.

Evans, D. V. & Porter, R. 1997 Near-trapping of waves by circular arrays of vertical cylinders. *Appl. Ocean Res.* **19** (2), 83–99.

Hazard, C. & Lenoir, M. 1993 Determination of scattering frequencies for an elastic floating body. *SIAM J. Math. Anal.* **24** (4), 1458–1514.

Hazard, C. & Lenoir, M. 2002 Surface water waves. In *Scattering* (ed. R. Pike & P. Sabatier), pp. 618–636. Academic.

Hazard, C. & Loret, F. 2007*a* Generalized eigenfunction expansions for scattering problems with an application to water waves. *Proc. R. Soc. Edinburgh* **137A**, 995–1035.

Hazard, C. & Loret, F. 2007*b* The singularity expansion method applied to the transient motions of a floating elastic plate. *Math. Modelling Numer. Anal.* **41** (5), 925–943.

Hazard, C. & Meylan, M. H. 2007 Spectral theory for a two-dimensional elastic thin plate floating on water of finite depth. *SIAM J. Appl. Math.* **68** (3), 629–647.

Ikebe, T. 1960 Eigenfunction expansions associated with the Schroedinger operators and their applications to scattering theory. *Arch. Ration. Mech. Anal.* **5**, 1–34.

Kagemoto, H. & Yue, D. K. P. 1986 Interactions among multiple three-dimensional bodies in water waves: an exact algebraic method. *J. Fluid Mech.* **166**, 189–209.

Linton, C. M. & Evans, D. V. 1990 The interaction of waves with arrays of vertical circular cylinders. *J. Fluid Mech.* **215**, 549–569.

Maskell, S. J. & Ursell, F. 1970 The transient motion of a foating body. *J. Fluid Mech.* **44**, 303–313.

McIver, M. 1996 An example of non-uniqueness in the two-dimensional water wave problem. *J. Fluid Mech.* **315**, 257–266.

McIver, M. 2000 Trapped modes supported by submerged obstacles. *Proc. R. Soc.* A **456**, 1851–1860.

McIver, P. & McIver, M. 1997 Excitation of trapped water waves by the forced motion of structures. *J. Mech. Appl. Math.* **50**, 165–178.

McIver, P. & McIver, M. 2006 Trapped modes in the water-wave problem for a freely-floating structure. *J. Fluid Mech.* **558**, 53–67.

Meylan, M. H 2002 Spectral solution of time dependent shallow water hydroelasticity. *J. Fluid Mech.* **454**, 387–402.

Meylan, M. H. & Gross, L. 2003 A parallel algorithm to find the zeros of a complex analytic function. *ANZIAM J.* **44** (E), E216–E234.

Povzner, A. Ya. 1953 On the expansions of arbitrary functions in terms of the eigenfunctions of the operator $-\Delta u + cu$ (in Russian). *Mat. Sbornik* **32** (74), 109–156.

Steinberg, S. 1968 Meromorphic families of compact operators. *Arch. Ration. Mech. Anal.* **31**, 72–379.

Ursell, F. 1964 The decay of the free motion of a floating body. *J. Fluid Mech.* **19**, 303–319.

Wilcox, C. H. 1975 *Scattering Theory for the d'Alembert Equation in Exterior Domains*. Springer-Verlag.

Yilmaz, O. & Incecik, A. 1998 Analytical solutions of the diffraction problem of a group of truncated vertical cylinders. *Ocean Engng* **25**, 385–394.